Supplementary Information for

Electrically Driven Plasmonic Lasing with Record-low Threshold

Baoqin Mu[1], Zelan Tang[1], Peiwei Si[1], Yao Yang[1], Lei Cheng[1], Ziyi Zhou[1], Ziqiu Chen[1], Bowen Liu*

[1]College of Chemistry and Chemical Engineering, Lanzhou University, Lanzhou 730000, China

*Correspondence to: lbw@lzu.edu.cn

Table of Contents

Supplementary Note 1 | Measurement and calculation of EQE for LEDs and integrated devices

The external quantum efficiency of the electroluminescent-driven LED and the integrated device was measured using a self-built platform. By adjusting the drive voltage, the luminescence behavior under different current densities was systematically investigated. Additionally, the external quantum efficiency (EQE) was measured in a darkroom by comparing the number of injected electrons to the number of emitted photons: A DC power supply (eTM-305SPD) scanned the voltage range from 16.6 V to 19.5 V in 0.1 V increments. Simultaneously, optical power data was collected using an optical power meter (PM100D, S120VC), enabling the calculation of the corresponding EQE values.

Number of injected electrons (Ne): By progressively altering the drive voltage and recording the corresponding current values (I), the number of electrons injected at each voltage can be calculated based on the relationship between current and elementary charge (q). The expression is:

$$N_e = \frac{I}{q} \tag{S1-1}$$

Number of Photons Emitted (Np): While adjusting the voltage, the light emitted by the device is collected by an integrating sphere and measured by a power meter at the light output port to determine the optical power (Popt). Combining this with the photon energy (Ephoton = hc/λ, where h is Planck's constant, c is the speed of light, and λ is the LED's emission wavelength), the number of emitted photons can be calculated:

$$N_P = \frac{P_{opt}}{E_{photon}} \tag{S1-2}$$

External Quantum Efficiency (EQE): Based on the injected electron count (Ne) and output photon count (Np) obtained above, the external quantum efficiency of the device can be further calculated, defined as:

$$\mathrm{EQE} = \frac{N_p}{N_e} \tag{S1-3}$$

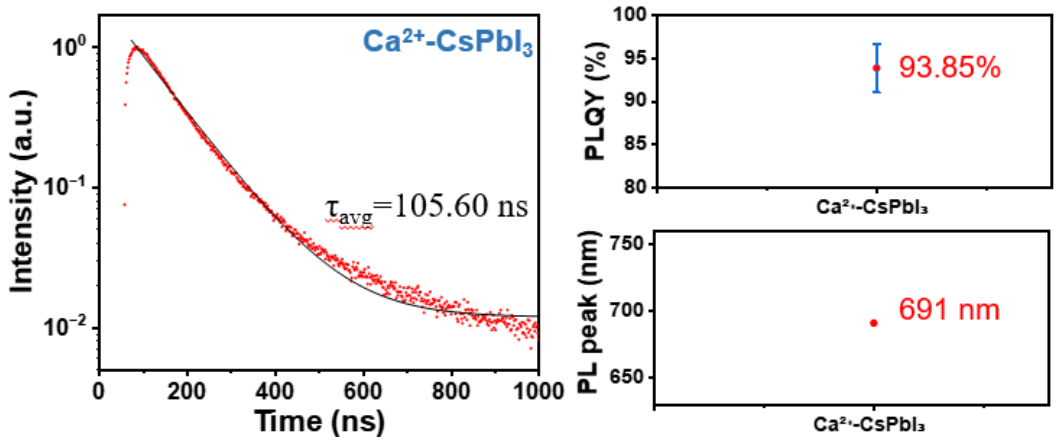

Supplementary Fig. 1 | Lifetime, photoluminescence quantum yield (PLQY), and emission wavelength center of perovskite gain medium (Ca^{2+}-$CsPbI_3$).

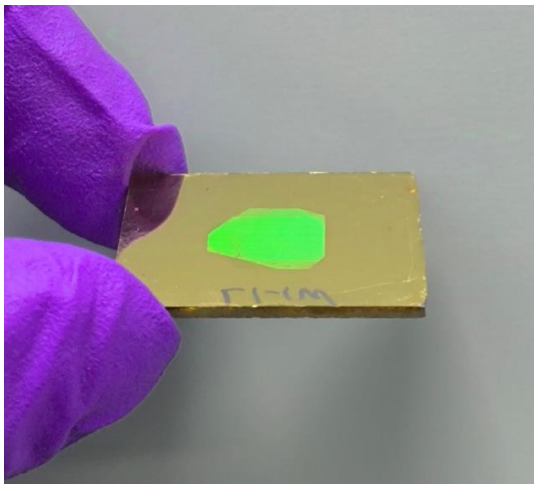

Supplementary Fig. 2 | Physical image of gold nanoparticle arrays fabricated using holographic lithography technology.

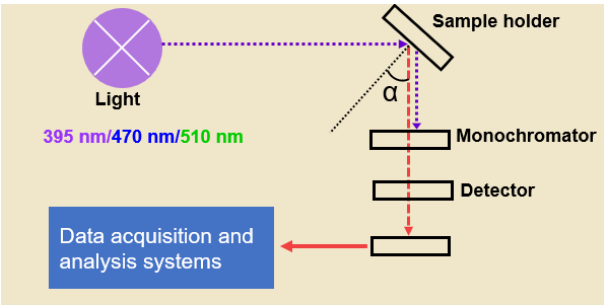

Supplementary Fig. 3 | TRPL test optical path.

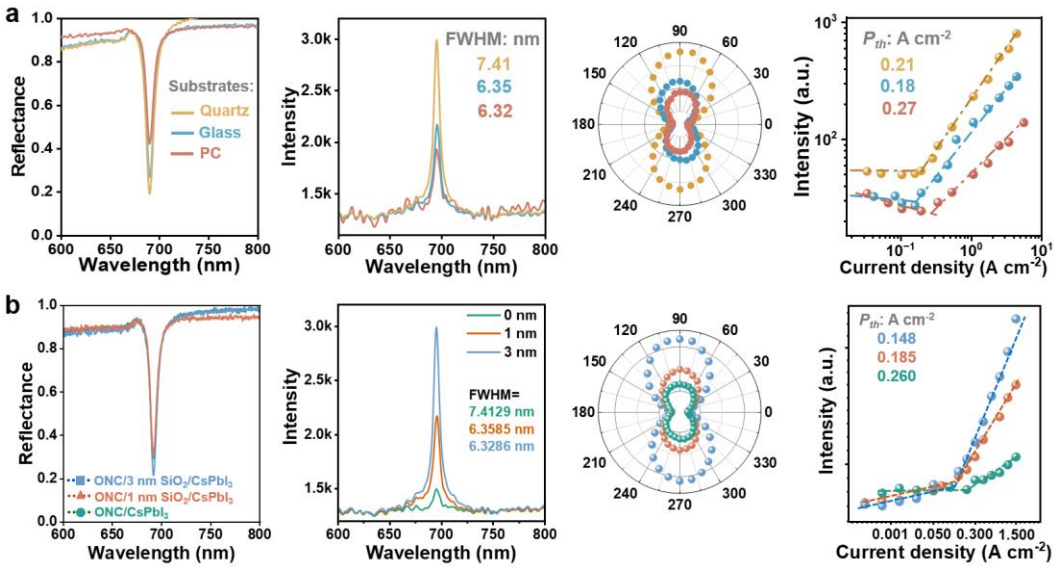

Supplementary Fig. 4 | Optimization study on substrate and silicon dioxide spacer layer thickness. a, Comparative analysis of the effects of different substrate materials (quartz, glass, and flexible polycarbonate (PC)) on plasmonic cavity performance, including SPR reflectance spectra, lasing spectra, polarization characteristics, and threshold changes. **b,** Performance comparison after introducing SiO_2 spacers of varying thicknesses between the plasmonic cavity and gain medium (Ca^{2+}-$CsPbI_3$), including SPR reflection spectra, lasing spectra, polarization, and threshold changes. This design aims to suppress the inherent metallic losses of plasmonic structures.

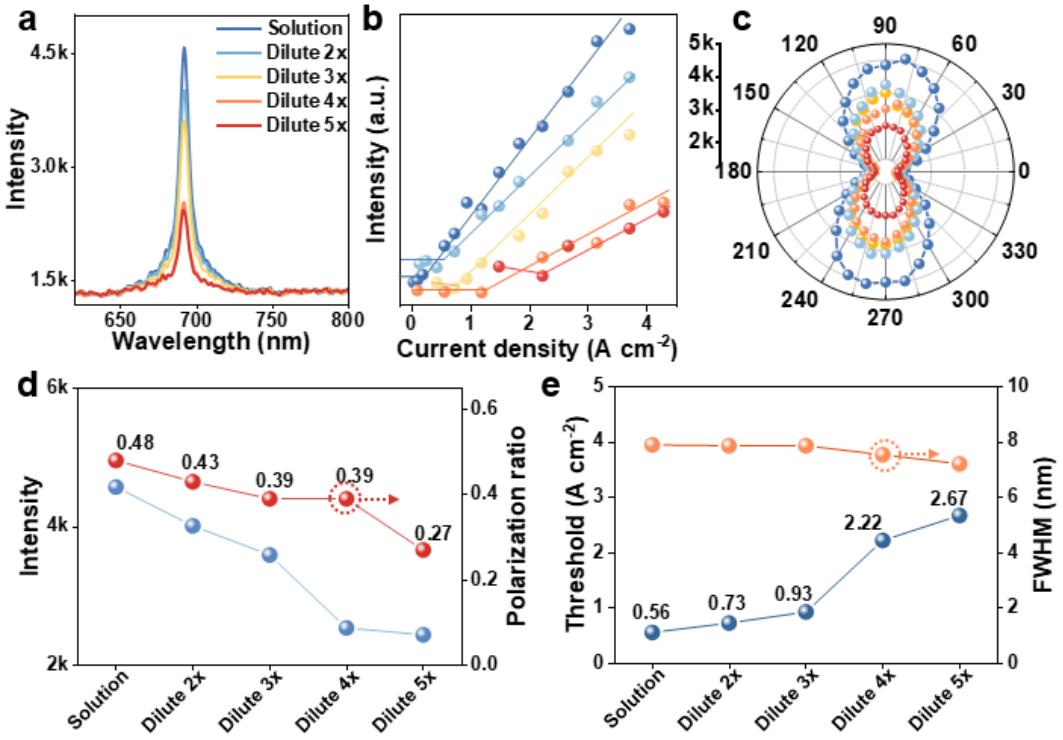

Supplementary Fig. 5 | Optimization of perovskite solution concentration under electro-driving conditions. a-c, Comparison of electro-drived laser properties for Ca^{2+}-$CsPbI_3$ at different concentrations: **(a)** laser emission spectrum, **(b)** threshold and **(c)** polarization characteristics. **d-e,** Concentration-dependent laser performance parameters: **(d)** threshold and FWHM, and **(e)** peak intensity versus polarization ratio.

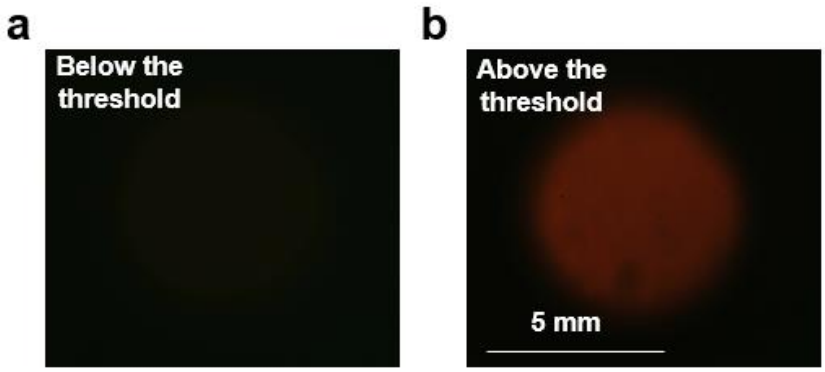

Supplementary Fig. 6 | Spots below the threshold and spots above the threshold.

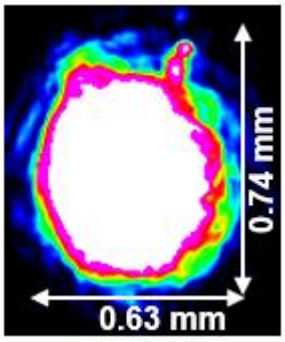

Supplementary Fig. 7 | 405 nm CW pump light spot.

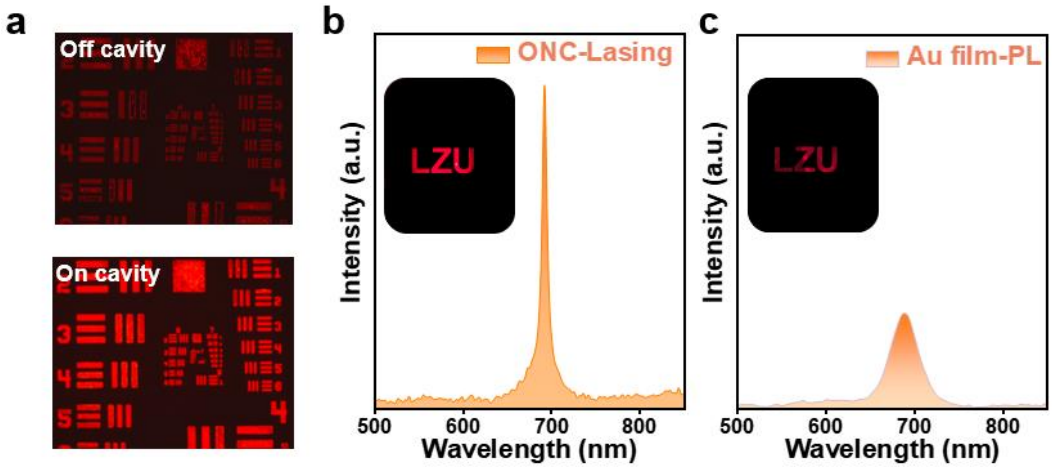

Supplementary Fig. 8 | Comparison of perovskite spin-coated on Au film versus ONC. a, Evaluation of perovskite laser imaging performance using the 1951 U.S. Air Force (AF) resolution test chart: Without a plasmonic cavity, the image appears overall dim with significant speckle. Introduction of the plasmonic cavity markedly enhances image clarity while substantially reducing speckle. This improveea3ment stems from the plasmonic laser's low spatial coherence effectively mitigating interference effects. **b-c,** Comparison of spectral and far-field imaging results. The brightness and clarity of images in laser imaging mode significantly outperform those in conventional fluorescence imaging mode, demonstrating the system's potential for enhanced performance in high-quality imaging applications.

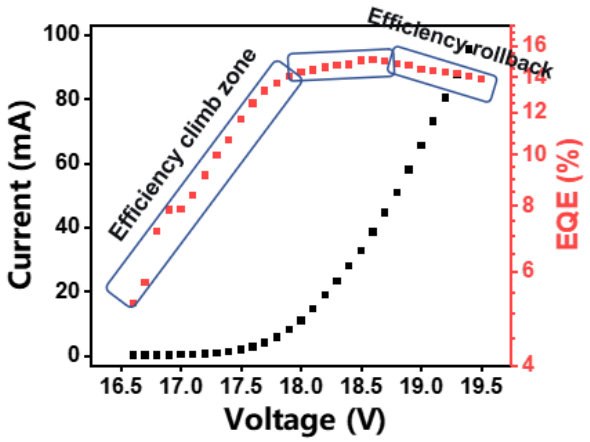

Supplementary Fig. 9 | Current-voltage (I-V, black) and external quantum efficiency-voltage (EQE-V, red) characteristics of the electroluminescent unit. The device achieved a maximum optical power of 39 mW under drive conditions, corresponding to an external quantum efficiency of 15.058%. Further enhancing its electro-optical conversion efficiency holds promise for enabling more efficient laser emission in this structure.

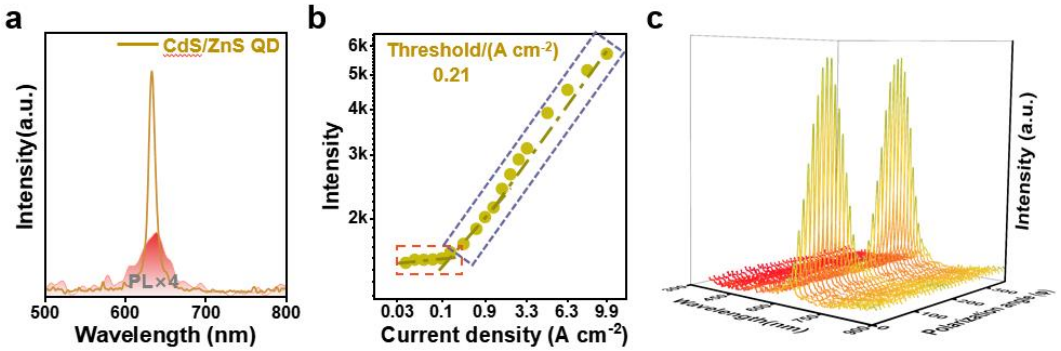

Supplementary Fig. 10 | Verification of the universality of the electrically driven approach. a, Narrow-linewidth emission spectra obtained under 405 nm LED integrated electrically driven illumination, with the gain medium replaced from Ca^{2+}-$CsPbI_3$ NCs to CdS/ZnS quantum dots, using the same integrated structure. **b,** Relationship between spectral output intensity and increasing drive current density. **c,** Relationship between output spectral intensity and polarization angle.